DNA Conformational Behavior and Compaction in Biomimetic Systems: Toward Better Understanding of DNA Packaging in Cell

Anatoly Zinchenko

Graduate School of Environmental Studies, Nagoya University, Furo-cho, Chikusa-ku, Nagoya, 464-8601, Japan

E-mail: zinchenko@urban.env.nagoya-u.ac.jp

Tel: +81-052-789-5629

Abstract

In a living cell, long genomic DNA is strongly compacted and exists in the environment characterized by a dense macromolecular crowding, high concentrations of mono- and divalent cations, and confinement of *ca.* 10 μm size surrounded by a phospholipid membrane. Experimental modelling of such complex biological system is challenging, but important to understand spatiotemporal dynamics and functions of the DNA in cell. The accumulated knowledge about DNA condensation/compaction in conditions resembling those in the real cell can be eventually

used to design and construct partly functional “artificial cells” having potential applications in drug delivery systems, gene therapy, and production of synthetic cells. In this review, I would like to overview the past progress in our understanding of the DNA conformational behavior and, in particular, DNA condensation/compaction phenomenon and its relation to the DNA biological activity. This understanding was gained by designing relevant experimental models mimicking DNA behavior in the environment of living cell. Starting with a brief summary of classic experimental systems to study DNA condensation/compaction, in later parts, I highlight recent experimental methodologies to address the effects of macromolecular crowding and nanoscale and microscale confinements on DNA conformation dynamics. All the studies are discussed in the light of their relevance to DNA behavior in living cells, and future prospect of the field are outlined.

Keywords DNA condensation and compaction; crowding; confinement; artificial cell; single-molecule

Contents of paper

6. Conclusions and outlook

1. Introduction

In a living cell, genomic DNA has to be strongly compacted to be accommodated within a confinement of micrometer size; therefore, the problem of DNA condensation (also referred to as "DNA folding" or "DNA compaction" for a single-molecule event) has attracted a considerable attention and has been rigorously studied for several decades. Experimental and theoretical studies on DNA condensation began in early 70s of the past century. Since then a broad variety of experimental techniques was utilized to understand physical principles underlying DNA condensation and factors controlling DNA condensation *in vivo* and *in vitro*. The timeline in **Figure 1** shows the appearance of various *in vitro* experimental model systems aimed to make clear DNA packaging in cells. Most of early studies focused on DNA phase behavior in solutions of polyamines and other cationic chemicals. Meanwhile, studies on DNA condensation in concentrated solutions of neutral macromolecules and salt were initiated to address the effect of molecular crowding in cell. The progress in development of microscopic techniques in 90s made possible single-molecule visualization of DNA conformational dynamics and folding/unfolding transitions and a more accurate interpretation of DNA compaction phenomenon.

However, in order to construct a more realistic experimental systems to model DNA behavior in the real cell, additional factors relevant to intercellular environment (**Figure 2)**, must be taken into account. The crucial ones are the following: (i) the presence of DNA condensing species interacting with negatively-charged DNA predominantly by electrostatic mechanism, (ii) the presence of high concentrations of low-molecular weight electrolytes such as NaCl and $MgCl_2$ in

solution, (iii) macromolecular crowding, and (iv) the influence of cell-sized microconfinement, in which DNA is placed. Ideally, all these factors should be considered simultaneously in a single experimental system; however, due to its obvious complexity, experimental design of such sophisticated system is a big challenge. During the past decade, along with new important experimental findings in (iii) and (iv) directions, there was a number of attempts to investigate the combined effect of two, three, or even four of above factors on DNA conformational behavior in a single model system. In this review, following the timeline in **Figure 1,** first, I briefly overview DNA condensation/compaction starting from pioneering studies. Earlier studies on DNA condensation/compaction are well reviewed in past literature, therefore, here I mainly provide references to the corresponding review articles. In the later parts, I discuss recent progress in the analysis of the combined effect of all factors (i) – (iv) on DNA behavior. It should be mentioned that length of genomic DNA in cells is on the order of several meters (eukaryotes), therefore, I limit this review to studies focused on high-order structure of long DNA molecules of length exceeding hundreds of kilobase pairs unless otherwise mentioned.

2. Compaction of DNA by positively charged molecules and colloids

In cells, condensation of negatively-charged DNA is assisted by its interaction with cationic species of various charge and structure [1]. Earliest experimental *in vitro* models of DNA compaction utilized multivalent cations such as organic polyamines (spermine, spermidine, etc.) or cationic transition metal complexes (hexamine cobalt) [2, 3]. DNA compaction was shown to occur as a result of neutralization of anionic charges on DNA macromolecule [4, 5] which is largely promoted by ion correlation effect, i.e. attraction between like-charged DNA segments mediated by multivalent cations [6, 7]. At the point of 89-90% neutralization/screening of the DNA charge, short range attractive forces overcome residual Coulombic repulsion resulting in DNA

collapse [2, 8]. Importantly, calorimetry studies demonstrated that binding of multivalent cations to DNA and subsequent DNA condensation are driven exclusively by the entropy contribution associated with the release of monovalent cations from DNA [9, 10].

Experimentally, compaction of DNA was studied as either DNA phase separation, i.e. precipitation of DNA from solution or as a transition from an elongated state to a very compact globule state at the level of single DNA molecule (**Figure 3**). Mono- and divalent cations do not induce DNA condensation in aqueous solutions because they are unable to sufficiently neutralize DNA charge [5]. Ion-exchange between monovalent and multivalent cations during DNA compaction contributes to stabilization of DNA compact state through an increase of translation entropy due to release of a large number of condensed monocations [11]. Compaction of DNA by multivalent cations having 3-9 cationic groups proceeds as all-or-none (discontinuous) type of DNA higher-order structural transition as illustrated by **Figure 3** on the example of spermine [11, 12]. In contrast, compaction of DNA by cationic species with higher charge such as polylysine, polyarginine and other polycations was shown to be a continuous process [13] characterized by gradual shrinking of DNA coil followed by DNA collapse (**Figure 4**). In the former case, discrete transition of DNA conformation is explained by similar stability of DNA coil and globule conformations in the intermediate range of multication concentrations when a large excess of multivalent cations is present in solution. In the latter case, however, polycations adsorb on DNA and induce its gradual compaction by cross-linking multiple DNA segments. DNA compaction by weak cationic binders is inhibited by monovalent cations and DNA condensates formed as a result of DNA compaction by weak cationic agents can be reversibly unfolded (decompacted) by adding monovalent cations [14]. Due to significant rigidity of the double-stranded DNA (the persistence length is *ca.* 50 nm in the physiological conditions) DNA is usually compacted DNA into

characteristic toroidal shape condensates of high density [15], in which DNA biological activity (e.g. transcription) is completely inhibited [16].

In the above studies, size and shape effects of DNA binders were usually neglected because of their small size. In the real cell, however, the DNA molecule frequently encounters cationic binders and surfaces of the nanoscale dimension [17] and due to the semi-flexible nature of DNA macromolecule its conformational behavior is greatly affected by the geometry of interacting species. In eukaryotic cells, for instance, DNA is folded by cationic proteins, histones, of *ca.* 7 nm size and then hierarchically assembled into chromosome gaining over 1000-fold compaction [18]. In order to model this type of DNA condensation, cationic dendrimers [19, 20], and nanoparticles (NP) [21, 22], were tested as model systems with a particular focus on their size and charge effects on DNA condensation/compaction. Zinchenko et al. studied DNA compaction by cationic nanoparticles with sizes from 10 to 100 nm and similar surface charge density (2-3 charges per square nm) and showed that the mode of DNA interaction with such cationic nanotemplates and DNA compaction degree strongly depend on their size as illustrated in **Figure 5**. Due to DNA stiffness at the nanoscale, interaction of DNA with small size and/or low cationic charge NP results in decorating of DNA macromolecule with colloidal particles. When either size or cationicity of NP increases, electrostatic attraction between DNA and cationic species overcomes the DNA bending stress penalty, and DNA molecule wraps around the cationic particle. The case of even larger cationic templates with sizes greater than 50 nm is similar to DNA adsorption on flat cationic surfaces. Murata et al. studied the effect of mono- and divalent cations on DNA compaction by small (10 nm) and large (100 nm) cationic nanoparticles [23, 24]. DNA compaction was most efficient in terms of nanoparticles concentration at intermediate salt concentrations that roughly correspond to the physiological salt conditions (*ca.* 0.1 M of NaCl). The decrease in DNA

compaction efficiency by NP in low salt is caused by the increase of DNA chain bending energy cost to form electrostatic complex with nanoparticles as well as by the strengthening of repulsing interactions between like-charged DNAs adsorbed on nanoparticle surface. On the other hand, at high concentrations of salt, electrostatic interactions between DNA and cationic NP are strongly screened that results again in inefficient DNA compaction.

In contrast to the abrupt and discontinuous coil-globule transition of DNA in solutions of multivalent cations, DNA compaction by nanosized colloidal particles of any sizes between 10 and 100 nm was continuous DNA folding likewise the DNA compaction by linear polycations. The difference between DNA compaction scenarios affects the way how DNA biological activity changes during DNA compaction event. For example, the multivalent cation spermine inhibits DNA transcription activity completely in a very narrow range of spermine concentrations preceding DNA collapse [16] due to an abrupt change of DNA conformation from unfolded and well accessible for binding proteins to very compact and thus inactive. In contrast, cationic NP induce step-by-step compaction of DNA coil and cause gradual inhibition of transcription as more sites on DNA molecule become “blocked” with strongly bound NP [25]. The inhibition is more cooperative and abrupt in the case of smaller nanoparticles as they resemble multication.

3. DNA compaction in crowded environment of neutral and anionic crowders

Whereas electrostatic interaction of DNA with cationic species is the predominant driving force of DNA condensation *in vivo*, construction of DNA-containing biomimetic systems is impossible without considering the high degree of macromolecular crowding in the real cell. Living cells contain 20-40% (w/w) of polymeric species [26, 27] and it has biochemical and

biophysical consequences for DNA higher-order structure and functions [28]. As a result, macromolecular crowding plays crucial role in a wide range of DNA-involved biological reactions [29]. In particular, the increased binding of DNA polymerase to DNA [30], promotion of DNA replication [31], promotion of DNA hybridization [32], enhancement of DNA hydrolysis by nucleases [33], etc. under crowding were reported.

In his pioneering study, Lerman addressed the influence of the crowded environment on DNA phase behavior by mixing it with neutral polymers such as polyethylene glycol (PEG) and salt at a high concentration [34]. It was found that DNA undergoes collapse into very compact particles in solutions containing about 10% (v/v) of neutral polymer and about 0.3 M of NaCl. This type of DNA compaction is referred to as Ψ (PSI = polymer and salt induced) DNA condensation. Ψ condensation of DNA is caused by non-miscibility of DNA and neutral polymer leading to the appearance of depletion attractions forces between DNA segments that ultimately results in DNA compaction. High concentrations of simple salt in solution efficiently suppress the DNA electrostatic charge and promote DNA condensation. Importantly, these experiments demonstrated that DNA adopts compact conformation in crowded environment and that DNA compaction can be realized even in solutions containing no cationic binders.

At the level of single molecule, DNA compaction in concentrated solutions of neutral polymers was shown to proceed similarly to DNA compaction by multivalent cations (**Figure 3**), i.e. as all-or-none folding transition from an elongated coil state to a compact globule state [35]. At a constant polymer volume fraction, this type of DNA compaction is promoted by an increase in neutral polymer length that contributes to to the value of the excluded volume as well as by an increase of salt concentration affecting a degree of DNA charge neutralization [35, 36]. By single molecule observations it was found that prior to DNA condensation in solutions of neutral

crowding agent dextran, the mobility DNA coil reduced drastically and DNA coil significantly elongated. The origin of this elongation is still poorly understood but assigned to a "complex interplay between entropic effects and crowder mobility" [37]. Both mentioned effects were much pronounced in solutions of higher molecular weight dextran. In tight condensates formed after DNA compaction the transcriptional activity of DNA was completely inhibited [16].

Mixing of DNA with anionic polymers and salt had similar effects on DNA conformational behavior as it was described for neutral crowders. The concentrations of polyanions such as polyglutamic acid, polyaspartic acid, or polyacrylic acid to induce either DNA precipitation [38] or single-molecule compaction [39] were reported to be of the same order as those found for neutral crowders, i.e. *ca.* 10-20% (w/v), and DNA compaction occurred as all-or-none coil-globule phase transition. Because in living cells macromolecules of different charges coexist, some studies attempted to address DNA conformational behavior in a mixture of crowders of different charges. In the solution of high concentrations of PEG, DNA folding and unfolding transitions induced by either a polycation or a polyanion, respectively, were shown to be greatly promoted in terms of critical concentration and cooperativity of DNA phase transition [40].

In earlier studies of DNA Ψ condensation, high molecular weight neutral polymers were utilized due to their significant excluded volume, but recently it was shown that DNA can be also compacted by negatively charged globular proteins and colloidal particles. Yoshikawa, Vasilevskaya et al. demonstrated that long chain single DNAs undergoe folding transition in solutions containing about 15% (w/v) of negatively-charged protein, bovine serum albumin (BSA), and salt [41-43]. Although BSA has positively charged fragments, due to its small size and high overall negative charge, DNA interaction with BSA can be considered as predominately repulsive. The origin of DNA phase transition induced by anionic globular species is essentially the same as

described for other crowders, i.e. depletion interactions, yet several unique features were noticed. For example, the dependence of DNA condensation by BSA on monovalent salt concentration was the opposite to the salt dependence of DNA condensation by neutral polymers due to the effect of salt on the excluded volume of polyanion. In the former case (**Figure 6**), addition of salt into solution of DNA and BSA results in screening of electrostatic charge of the polyanions. Consequently, the decrease of the Debye length of BSA causes the decrease of the excluded volume of polyanions and unfolding of DNA in a less crowded media. On the other hand, the excluded volume of a neutral crowder is not much influenced by fluctuation s of ionic strength, but because high concentration of salt promotes DNA charge neutralization, an increase of monovalent ions concentration in solution of a neutral polymer promotes DNA compaction.

Although small spherical crowders are less efficient depletion agents than flexible polymers, theoretical studies made clear the possibility of DNA compaction by small crowders in solutions of relatively low ionic strengths [44, 45]. Later, Zinchenko et al. studied DNA compaction by negatively charged silica nanoparticles of 20, 55, and to 135 nm size (zeta potential values are −25, −35, and −30 mV, respectively) under conditions of low salt, 1 mM of NaCl [46]. They showed that, similarly to DNA compaction by BSA, DNA undergoes compaction in concentrated solutions of anionic nanoparticles of any diameter. Threshold NP concentration in DNA compaction by large 135 nm nanoparticles was about 10% (w/v), but only 1% of small 20 nm nanoparticles was sufficient to compact DNA. The size effect of NP was discussed by taking into account the contribution of the Debye length to the total excluded volume of anionic nanoparticles. Obviously, relative increase of nanoparticles' excluded volume due to electrostatic interactions between DNA and NP ($(V_{NM}+l_d)/V_{NP}$, where l_d is Debye length) is more significant for smaller particles. The

recalculated total excluded volume of the nanospheres at the point of DNA compaction using Debye length was nearly the same and equal *ca.* 20% (w/v).

The crowded environment around DNA molecules does not only have a strong influence on the conformational behavior of DNA, but it also has a profound effect on DNA secondary structure. Stability of DNA double helix under crowded environment was studied by measuring DNA melting temperature at which DNA undergoes helix-coil transition resulting in separation of the double-helix into two single strands. In a majority of studies, addition of crowders to DNA solution resulted in stabilization of DNA duplexes and triplexes and accompanied by increase of DNA melting temperature [47-49]. Anionic crowders were shown to have stronger stabilization effect than neutral ones probably as a result of additional electrostatic contribution to the excluded volume effect [48]. However, destabilization of the DNA double-helix in solutions of PEG [50] and anionic spheres [46] was also reported. It was found that in PEG solutions strands exchange between double-stranded DNA was dramatically accelerated supporting the scenario of DNA denaturation under crowding [51]. The opposite effects of crowding on DNA double-strand stability are attributed to a large number of parameters involved such as decreased water activity, altered behavior of counterions, disruption of hydrogen bonds between DNA strands, etc., and contribution of each parameter can largely vary in every particular system depending on DNA length, crowder size, crowder charge, ionic strength, etc.

4. DNA conformational behavior in confined spaces

The size of the living cell (*ca.* 10 μm) is significantly smaller than it is required to accommodate the whole genomic DNA of *ca.* 3 meters length in its free unfolded state (human cell), hence the studies on DNA conformational behavior in a confined space are of particular

importance for understanding of factors controlling DNA condensation and accurate experimental modeling of DNA behavior inside living cells. Past studies on DNA behavior under confinement can be roughly divided into two groups: (i) the studies aimed at understanding of DNA conformational dynamics under extreme nano-confinement of 10-100 nm size, and (ii) the studies that were performed to make clear the DNA behavior in the cell-sized space (10-100 μm) surrounded by a phospholipid membrane to construct *in vitro* biomimetic cell models, so-called "artificial cells".

4.1 DNA conformational dynamics in nanoslits and nanochannels

During the past decade, two-dimensional nanoslit and one-dimensional nanochannel confinements were actively utilized for visualization of DNA conformational behavior by fluorescent microscopy technique under nano-confinement in aqueous solution and in the presence of DNA binders. Confinement of DNA molecules in a nanoslit represents a transition from 3-dimentional to quazi-2-dimentional regime. In solutions without DNA binders, the confinement of DNA in a slit results in the increase in the DNA coil size, which depends on nanoslit height. Ichikawa et al. showed that there is a characteristic height of the slit confinement that separate 3-dimentional and quazi-2-dimensional regimes [52]. This characteristic height corresponds to the Flory radius of DNA coil, i.e. 4.45 μm for T4 DNA (165 kbp) of 65 μm contour length. **Figure 7** shows that under the confinement with the height smaller than the Flory radius of DNA (i.e. in 2-dimensional regime) the average long-axis length of DNA coils progressively increases with the decrease of slit height. Doyle et al. studied conformational behavior of λ-DNA (48 kbp) [53] in 2-dimensional confinement in a broad range of heights from 32 nm to 10 μm and reported similar two-regime dependence. Gyration radius of λ-DNA coil was constant under confinement's height

larger than 2 μm and almost equal to the gyration radius of DNA coil in a bulk solution, while it increased monotonically in lower heights regime. Under 32 nm confinement the gyration radius of DNA was nearly doubled in comparison to unconfined DNA in a bulk solution. The increase of DNA coil size under 2-dimensional confinement was also accompanied by changes in DNA self-diffusion coefficients and rotational relaxation times. Lee et al. studied the effect of ionic strength on DNA conformation under strong nanoslit confinement and discussed the influence of ionic strength on DNA−DNA and DNA−nanoslit repulsion interactions and DNA conformation [54]. They performed systematic analysis of past experimental data reported in literature and concluded that the size of DNA confined in a slit depends on slit height, the DNA persistence length, and the effective diameter (swelling degree) of DNA.

Accompanied by recent progress in fabrication of micro- and nanofluidic devices, a number of experimental and theoretical studies of DNA conformational behavior in 1-dimensional nanochannel was also performed [55]. These studies are primarily motivated by a prospective practical application of DNA stretching in nanochannels for analysis of DNA genome. In a good agreement with the trends observed in nanoslits, in nanochannels DNA swelled and adopted even more extended coil conformation due to restrictions in its configurational degrees of freedom (**Figure 8**) [56, 57]. Decrease in the ionic strength of solution greatly promote the extension of DNA macromolecule due to stronger electrostatic repulsion interactions that increases the persistence length (rigidity) of DNA [58-60]. Under optimized condition, in 250 nm × 400 nm channel under low ionic strengths, long DNA molecules could be stretched almost to its full contour length, i.e. up to 88% of the contour length [61].

While DNA behavior in nanoslit and nanochannel confinements was intensively investigated, surprisingly, there are almost no studies focused on DNA interaction with cationic binders under confinement. As shown in **Figure 2**, DNA interaction with cationic binders under strong confinement is very relevant to the DNA binding to cationic proteins in cell nucleus and thus of great interest and importance. van der Maarel et al. studied the interaction of T4 DNA with cationic arginine-rich protein, protamine, in 200 nm × 300 nm nanochannel [62]. They found that DNA molecule was progressively compacted by protamine, and this compaction was more efficient in terms of polyamine threshold concentration as well as compaction kinetics at intermediate concentrations of salt (10 mM) (**Figure 9**). Unfortunately, the role of nanoconfinement itself in the process of DNA compaction was not addressed. In the same paper, they also studied the unfolding process of protamine-compacted DNA by adding NaCl and showed that compact DNA can be reversibly unfolded in the nanochannels in high ionic strength solution. The unfolding time increased with the increase of the concentration of coexisted with DNA protamine.

4.2 DNA confined in droplets, vesicles, and liposomes

A completely different direction in the research on DNA conformational behavior in the confined space was to address DNA behavior in the real cell and to construct primitive artificial cells [63]. Water droplets stabilized in oil by lipids and giant liposomes were chosen as suitable experimental models of living cell's confinement. The methods of their preparation as well as properties are currently being vigorously investigated [64]. These artificial models of cells have a characteristic size of the confinement on the order of 10-100 μm which is separated from outer solution by phospholipid layer. The charge of phospholipid membrane can be controlled in a broad

range by selecting suitable lipids for membrane construction, but it is usually constructed to possess negative charge in order to mimic living cell.

The possibility to entrap short DNA fragments into vesicles was demonstrated a long ago as a tool for gene transfer, [65, 66] yet no insight into conformational behavior of DNA in cell-sized confinement was provided. In 2000s Yoshikawa and colleagues initiated studies aimed at understanding of physico-chemical aspects of long DNA molecules behavior under cell-sized confinement. T4 phage DNA can be placed into a giant vesicles by natural swelling of phospholipid film in solutions containing DNA as shown in **Figure 10** [67]. DNA can be entrapped either in its unfolded coil conformation or in compact globular state after complexation, for instance, with histone proteins [68]. Baigl et al. studied conformational changes of single DNA molecules in cell-sized droplets and succeeded to control the conformation of encapsulated DNA photochemically with a help of photosensitive binder which DNA-binding character was reversibly switched by irradiation with a light of a certain wavelength [69]. Inside giant vesicles DNA preserves its biological activity and transcription reaction can be successfully performed in such "biochemical reactor" after encapsulating DNA with polymerase and other necessary chemicals [70, 71]. At present, post-addition and exchange of DNA or other chemicals after their encapsulation between the giant vesicles/droplets and outer solution are not possible; therefore, the solution of desired composition including chemicals for biochemical reactions is firstly prepared and then encapsulated into the microcontainers by natural swelling of phospholipid film, pipetting of DNA solution into oil, and other techniques [64]. Alternatively, an approach of direct transfer of compacted DNA one-at-a-time by laser tweezers from bulk solution into a giant vesicle was proposed [71].Size of the confinement in the above experimental models of cell (10-100 μm) is significantly larger than the confinement of nanoslits or nanochannels (*ca.* 50-500 nm), therefore,

a dramatic influence of DNA encapsulation on DNA conformation reported for nanoslits and nanochannels is generally not expected. On the other hand, it is important that the conformational behavior of DNA in cell-sized confinement of droplet/vesicle is greatly affected by the presence of a charged membrane at the interface of the confinement and outer solution. Cationic species interacting with negatively-charged DNA are also involved in the electrostatic interaction with phospholipid membrane composed of zwitterionic or anionic lipids. As a result, although the interaction of DNA and phospholipid membrane is not attractive, in the presence of multivalent cations inside the confinement DNA can adsorb on the surface of membrane [72]. For example, partitioning of T4 DNA in phospholipid membrane-coated droplets between internal solution and surface changed dramatically in the presence of magnesium ions and at 10 mM Mg^{2+} (physiological concentration) the entire encapsulated DNA was adsorbed onto the phospholipid membrane. The extent of this effect was shown to correlate with charge structure of lipid headgroup in the membrane [73]. In the same study, compaction of DNA by tetraamine, spermine, in the presence of Mg^{2+} of different concentrations in a bulk solution and inside the cell-sized confinement was compared. In the absence of Mg^{2+} ion, DNA compacted by spermine into globules exhibited Brownian motion inside droplets. When the concentration of Mg^{2+} was relatively high, encapsulation of compacted by spermine DNA resulted in the unfolding of DNA to coil conformation and adsorption of DNA coils onto the phospholipid membrane. Smaller size of droplets (20-80 μm) favored DNA adsorption onto phospholipid membrane (**Figure 11**), while in large droplets (80-200 μm) a large fraction of unfolded DNA was also partitioned in droplet..

Because in [73] two types of cationic species (Mg^{2+} and spermine) were used, it was difficult to deduce their individual roles. Therefore, recently, Hamada et al. studied the conformational behavior of T4 DNA in the presence of only trication spermidine (without Mg^{2+}) in 10 to 100 μm

water-in-oil droplets covered by phospholipids [74]. **Figure 12** shows the obtained phase diagram of T4 DNA in a bulk solution and in droplets of different sizes and at different spermidine concentrations together with the data of the DNA partitioning inside droplets. Adsorption of DNA on negatively-charged phospholipid surface is induced by the interaction of positively charged spermidine with membrane that turns DNA interaction with membrane to attractive. Consequently, at high concentration of spermine both unfolded and compact DNA molecules were exclusively observed on membrane. Importantly, the increase in droplet size at constant concentration of triamine resulted in conformational transition of adsorbed DNA from compact to unfolded conformation. This unfolding transition is explained by free energy changes during interplay between DNA coil-globule transition, DNA adsorption/desorption transition on/from membrane wall, and changes of ions translational entropy. When concentration of spermidine was low, DNA adopted coil confirmation regardless of droplet size, but while in smaller droplets unfolded DNA was located inside solution, DNA coils preferentially adsorbed on the membrane of larger ones.

Both [73] and [74] show that phospholipid membrane can induce unfolding of the compact DNA that might have very important consequences for DNA accessibility to proteins and activation of various biochemical reactions. On the other hand, the reported effects of droplet size on DNA adsorption on the confinement membrane in [73] and [74] are opposite, which is probably due to the presence of Mg^{2+} ion in the system described in [73]. Obviously, DNA conformational behavior and partitioning in cell-sized droplets are determined by a very delicate interplay of many parameters including concentration of DNA binders, ionic strength, droplet size, surface property of confinement membrane, etc., but further systematic studies are required to understand the whole picture.

The event of DNA encapsulation itself is sufficient to induce dramatic changes not only in DNA conformation but also in DNA biological functions. Encapsulation of DNA into cell-sized droplet was shown to result in remarkable acceleration of DNA gene expression, which was reversely proportional to the size of droplets [75]. The authors of [75] stressed that in such system both the size of the confinement and the presence of membrane surface affected gene expression. In particular, they tested a number of phospholipids and found that anionic character of the confinement membrane promoted the expression reaction at a larger extent.

5. Compaction of DNA under confinement and in the presence of crowders

Generally speaking, both macromolecular crowding and confinement contribute to the excluded volume around a macromolecule by exclusion of one soluble macromolecule by another or by a fixed boundary to the macromolecule, respectively. As it was discussed above, originally, the effects of macromolecular crowding and confinement on DNA conformational behavior were studied separately, but very recent experimental observations of DNA confined in nano-geometries and micro-geometries in the presence of crowders revealed a number of interesting features of the combined influence of both factors on DNA conformational dynamics.

Doyle, van der Maarel et al. studied DNA conformational behavior in the presence of electrostatically neutral dextran crowders of 3-17 nm size (R_g) in a bulk solution, under confinement of 2-dimentional nanoslit of 250 nm height, and 1-dimentional nanochannel of similar width and depth [76]. A drastic difference in the response of DNA conformation to the addition of crowder in these three systems was found. In unconfined bulk solution DNA coil size monotonically decreased with an increase of dextran concentration. Under nanoslit confinement, however, the change of DNA coil size became non-monotonic: with the increase of dextran

concentration DNA first swelled and then shrunk, yet the DNA collapse did not occur under 2-dimentional confinement. DNA conformational changed in 1-dimentional nanochannel was observed as gradual elongation of DNA coil at earlier stages followed by abrupt collapse of DNA coil into globule at high concentrations of dextran (**Figure 13A**) [77]. Because the elongation of DNA coil occurred only under confinement, it was attributed to the coupled effect of confinement and crowding. Swelling of DNA coil in such systems was explained as a result of osmotic pressure working in the inward direction of the nanochannel caused by depletion of dextran density in the interior of DNA coil in comparison to dextran concentration near channel walls. Due to the stronger confinement in nanochannels, i.e. presence of four walls around DNA limiting its degree of freedom, the osmotic pressure and the extent of DNA coil elongation in nanochannels were significantly larger than under nanoslit confinement. For example, at the point of the maximum DNA coil extension *ca.* 40% and *ca.* 14% DNA elongation was observed in nanochannels and nanoslits, respectively. In the above studies it was successfully revealed that strong confinement of DNA promote DNA condensation in a crowded environment. Furthermore, it was demonstrated for the first time that DNA can undergo compaction in solutions of crowders almost without added salt (c(NaCl) = 3 mM), whereas in the classic Ψ (PSI = polymer and salt induced) condensation scenario, the coexistence of high concentrations of salt was the indispensable condition to induce DNA charge neutralization and compaction.

To address the influence of electrostatic charge of crowder, DNA conformation in nanochannels was also analyzed in the presence of anionic BSA protein [77], which is of similar size to dextran but has a negative charge of *ca.* −15 per molecule at pH 8.5. In contrast to DNA coil swelling induced by neutral dextran in nanochannels, compaction of DNA by BSA in nanochannels preceded by contraction of DNA coil due to the predominant role of repulsive

interactions between like-charged BSA and DNA (**Figure 13B**). Critical concentration of crowder to induce DNA compaction shifted to higher values in narrower channels and DNA compaction was shown not to occur in the narrowest 60 × 100 nm^2 channel at any concentration of BSA. As a result of change in nanochannel's width from 300 × 250 nm^2 to 100 × 250 nm^2, about 10-fold increase in BSA concentration to induce DNA compaction was observed.

To address DNA conformational behavior inside cell-sizes confinement under crowding, Yoshikawa et al. studied phase separation of relatively short 300-700 bp DNA in concentrated PEG solution inside water-in-oil droplets of 50-170 μm size [78]. They found that DNA phase separation can take place under confinement of droplet even when no DNA condensation is observed in a bulk solution containing the same quantities of DNA and PEG. In a good agreement with previous reports, the event of DNA phase separation occurs at the interface of the droplet, where the ordered condensed phase of DNA is formed. In droplets of smaller size DNA phase separation was significantly promoted.

Later, studies on T4 DNA conformational behavior inside phospholipid-coated droplets were performed in the presence of anionic crowders of different rigidity and the influence of crowder concentration as well as size of the confinement on DNA conformation and partitioning inside droplets were reported [79, 80]. In these studies, DNA was taken at concentrations much higher than in single-molecule experiments, i.e. 0.34 mg/mL. Sodium alginate, an anionic polysaccharide, was used as a semi-flexible anionic crowder (persistence length = 5 nm). In bulk solution containing 0-0.5% of alginate, the size of DNA coil progressively decreased with an increase of anionic crowder concentration. **Figure 14** shows phase diagram of the DNA conformational state and partitioning inside micrometer size droplet. At low concentrations of alginate DNA

condensation occurred mostly inside the confinement space, but at higher concentrations of the crowder, all the condensed DNA molecules adsorbed on the phospholipid membrane of the droplets. In the confinement of smaller size, *ca.* 10 μm, DNA tended to condense more efficiently. Similar phase behavior was found in mixtures of concentrated DNA and highly rigid polyanion, actin (persistence length *ca.* 10 μm), encapsulated into the microdroplets [79]. Both DNA and actin tended to condense under conditions of strong confinement and to adsorb on the membrane of droplets. In droplets of larger sizes (> 20 μm), phase separation scenarios of DNA and actin depended strongly on the concentration of actin inside droplets. At low concentrations of actin, both polyanions were dispersed inside the droplets, but when the concentration of actin increased, DNA selectively precipitated on droplets' membrane and only actin remained inside the droplets. Adsorption of actin on the membrane of droplets was favored only under very strong crowding (high actin concentrations), at which both DNA and actin were excluded toward the surface of phospholipid membrane.

6. Conclusions and outlook

Although earlier experimental models of DNA condensation/compaction reported since 1970s made clear fundamental aspects of DNA condensation induced in solutions of cationic species or in highly concentrated mixtures of polymers and salt, all those models focused primarily on one or two system parameters among those shown in **Figure 2**. In present, DNA conformational behavior in such simple systems is no more considered to reflect the actual DNA behavior in the living cell. New experimental model systems reported during past 15 years of progress in this field address more realistic biomimetic scenarios of DNA condensation and reveal new striking features of DNA condensation/compaction. In particular, DNA condensation phenomenon was found to be

largely affected by the size of the confinement where the DNA condensation event occurs. Furthermore, DNA condensation inside the microdroplets mimicking the real cell environment was shown to be influenced not only by the size of the droplet but also by the surface state of phospholipid membrane that can trigger DNA conformational changes in the vicinity of the confinement wall. However, the number of reports describing these new systems is still relatively small, and even fewer is the number of systematic studies. More comprehensive and functional systems should be constructed and explored to make clear how DNA interaction with cationic species takes place inside a confined micrometer-sized space in the presence of high concentrations of macromolecular crowders. For example, all DNA condensation/compaction systems described here show strong dependence on the ionic strength of media, which can either promote or impede DNA condensation depending on a condensation scenario. Therefore, in the systems consisting of multiple components that can induce DNA condensation independently, slight change in simple salt concentration may result in a highly cooperative phenomena of DNA folding/unfolding. Because many biological functions of DNA are intimately related to the degree of DNA condensation that can be dramatically altered under confinement, macromolecular crowding, etc., the applications of new experimental model systems for DNA condensation in biological and biomedical fields are also awaited. Finally, although probably futuristic, further development and optimization of liposome-encapsulated DNA systems, might ultimately allow to create first functional synthetic cells.

Acknowledgements

I would like to sincerely thank Prof. Kenichi Yoshikawa (Doshisha University, Japan) for introducing me to the exciting field of DNA compaction, 15 years of close collaboration, and encouragement.

References

[1] Teif VB, Bohinc K. Condensed DNA: condensing the concepts. Progress in biophysics and molecular biology. 2011;105:208-22.

[2] Bloomfield VA. DNA condensation. Curr Opin Struc Biol. 1996;6:334-41.

[3] Estevez-Torres A, Baigl D. DNA compaction: fundamentals and applications. Soft Matter. 2011;7:6746-56.

[4] Wilson RW, Bloomfield VA. Counter-Ion-Induced Condensation of Deoxyribonucleic-Acid - Light-Scattering Study. Biochemistry-Us. 1979;18:2192-6.

[5] Arscott PG, Ma CL, Wenner JR, Bloomfield VA. DNA Condensation by Cobalt Hexaammine(Iii) in Alcohol-Water Mixtures - Dielectric-Constant and Other Solvent Effects. Biopolymers. 1995;36:345-64.

[6] Khan MO, Mel'nikov SM, Jonsson B. Anomalous salt effects on DNA conformation: Experiment and theory. Macromolecules. 1999;32:8836-40.

[7] Khan MO, Jonsson B. Electrostatic correlations fold DNA. Biopolymers. 1999;49:121-5.

[8] Bloomfield VA. DNA condensation by multivalent cations. Biopolymers. 1997;44:269-82.

[9] Matulis D, Rouzina I, Bloomfield VA. Thermodynamics of DNA binding and condensation: Isothermal titration calorimetry and electrostatic mechanism. J Mol Biol. 2000;296:1053-63.

[10] Korolev N, Berezhnoy NV, Eom KD, Tam JP, Nordenskiold L. A universal description for the experimental behavior of salt-(in)dependent oligocation-induced DNA condensation (vol 37, pg 7137, 2009). Nucleic Acids Res. 2012;40:2807-21.

[11] Takahashi M, Yoshikawa K, Vasilevskaya VV, Khokhlov AR. Discrete coil-globule transition of single duplex DNAs induced by polyamines. J Phys Chem B. 1997;101:9396-401.

[12] Yoshikawa K, Takahashi M, Vasilevskaya VV, Khokhlov AR. Large discrete transition in a single DNA molecule appears continuous in the ensemble. Phys Rev Lett. 1996;76:3029-31.

[13] Akitaya T, Seno A, Nakai T, Hazemoto N, Murata S, Yoshikawa K. Weak interaction induces an ON/OFF switch, whereas strong interaction causes gradual change: Folding transition of a long duplex DNA chain by poly-L-lysine. Biomacromolecules. 2007;8:273-8.

[14] Hibino K, Yoshikawa Y, Murata S, Saito T, Zinchenko AA, Yoshikawa K. Na+ more strongly inhibits DNA compaction by spermidine (3+) than K+. Chem Phys Lett. 2006;426:405-9.

[15] Hud NV, Downing KH. Cryoelectron microscopy of lambda phage DNA condensates in vitreous ice: The fine structure of DNA toroids. P Natl Acad Sci USA. 2001;98:14925-30.

[16] Tsumoto K, Luckel F, Yoshikawa K. Giant DNA molecules exhibit on/off switching of transcriptional activity through conformational transition. Biophys Chem. 2003;106:23-9.

[17] Zinchenko AA, Chen N. Compaction of DNA on nanoscale three-dimensional templates. J Phys-Condens Mat. 2006;18:R453-R80.

[18] Zlatanova J, Leuba SH. Chromatin fibers, one-at-a-time. J Mol Biol. 2003;331:1-19.

[19] Ottaviani MF, Furini F, Casini A, Turro NJ, Jockusch S, Tomalia DA, et al. Formation of supramolecular structures between DNA and starburst dendrimers studied by EPR, CD, UV, and melting profiles. Macromolecules. 2000;33:7842-51.

[20] Kabanov VA, Sergeyev VG, Pyshkina OA, Zinchenko AA, Zezin AB, Joosten JGH, et al. Interpolyelectrolyte complexes formed by DNA and astramol poly(propylene imine) dendrimers. Macromolecules. 2000;33:9587-93.

[21] Zinchenko AA, Sakaue T, Araki S, Yoshikawa K, Baigl D. Single-chain compaction of long duplex DNA by cationic nanoparticles: Modes of interaction and comparison with chromatin. J Phys Chem B. 2007;111:3019-31.

[22] Zinchenko AA, Yoshikawa K, Baigl D. Compaction of single-chain DNA by histone-inspired nanoparticles. Phys Rev Lett. 2005;95.

[23] Takenaka T, Zinchenko AA, Yoshikawa K, Murata S. Roles of Mono- and Divalent Cations in DNA Compaction Induced by Histone-Mimic Nanoparticles. B Chem Soc Jpn. 2010;83:643-50.

[24] Takenaka T, Zinchenko AA, Yoshikawa K, Murata S. DNA Compaction on Histone Mimics Prepared from Silica Nanoparticles. Chem Lett. 2010;39:72-3.

[25] Zinchenko AA, Luckel F, Yoshikawa K. Transcription of giant DNA complexed with cationic nanoparticles as a simple model of chromatin. Biophys J. 2007;92:1318-25.

[26] Zimmerman SB, Minton AP. Macromolecular crowding: biochemical, biophysical, and physiological consequences. Annual review of biophysics and biomolecular structure. 1993;22:27-65.

[27] Minton AP. Influence of macromolecular crowding upon the stability and state of association of proteins: Predictions and observations. J Pharm Sci-Us. 2005;94:1668-75.

[28] Miyoshi D, Sugimoto N. Molecular crowding effects on structure and stability of DNA. Biochimie. 2008;90:1040-51.

[29] Zhou HX, Rivas GN, Minton AP. Macromolecular crowding and confinement: Biochemical, biophysical, and potential physiological consequences. Annu Rev Biophys. 2008;37:375-97.

[30] Zimmerman SB, Harrison B. Macromolecular Crowding Increases Binding of DNA-Polymerase to DNA - an Adaptive Effect. P Natl Acad Sci USA. 1987;84:1871-5.

[31] Akabayov B, Akabayov SR, Lee SJ, Wagner G, Richardson CC. Impact of macromolecular crowding on DNA replication. Nat Commun. 2013;4.

[32] Baltierra-Jasso LE, Morten MJ, Laflor L, Quinn SD, Magennis SW. Crowding-Induced Hybridization of Single DNA Hairpins. J Am Chem Soc. 2015;137:16020-3.

[33] Sasaki Y, Miyoshi D, Sugimoto N. Regulation of DNA nucleases by molecular crowding. Nucleic Acids Res. 2007;35:4086-93.

[34] Lerman LS. Transition to a Compact Form of DNA in Polymer Solutions. P Natl Acad Sci USA. 1971;68:1886-&.

[35] Vasilevskaya VV, Khokhlov AR, Matsuzawa Y, Yoshikawa K. Collapse of Single DNA Molecule in Poly(Ethylene Glycol) Solutions. J Chem Phys. 1995;102:6595-602.

[36] Zinchenko AA, Yoshikawa K. Na+ shows a markedly higher potential than K+ in DNA compaction in a crowded environment. Biophys J. 2005;88:4118-23.

[37] Chapman CD, Gorczyca S, Robertson-Anderson RM. Crowding Induces Complex Ergodic Diffusion and Dynamic Elongation of Large DNA Molecules. Biophys J. 2015;108:1220-8.

[38] Laemmli UK, Paulson JR, Hitchins V. Maturation of the head of bacteriophage T4. V. A possible DNA packaging mechanism: in vitro cleavage of the head proteins and the structure of the core of the polyhead. Journal of supramolecular structure. 1974;2:276-301.

[39] Ichiba Y, Yoshikawa K. Single chain observation on collapse transition in giant DNA induced by negatively-charged polymer. Biochemical and biophysical research communications. 1998;242:441-5.

[40] Kidoaki S, Yoshikawa K. Folding and unfolding of a giant duplex-DNA in a mixed solution with polycations, polyanions and crowding neutral polymers. Biophys Chem. 1999;76:133-43.

[41] Krotova MK, Vasilevskaya VV, Makita N, Yoshikawa K, Khokhlov AR. DNA Compaction in a Crowded Environment with Negatively Charged Proteins. Phys Rev Lett. 2010;105.

[42] Yoshikawa K, Hirota S, Makita N, Yoshikawa Y. Compaction of DNA Induced by Like-Charge Protein: Opposite Salt-Effect against the Polymer-Salt-Induced Condensation with Neutral Polymer. J Phys Chem Lett. 2010;1:1763-6.

[43] Krotova MK, Vasilevskaya VV, Khokhlov AR. Compaction of DNA in solutions of highly charged proteins carrying the same charge as DNA. Polym Sci Ser C+. 2012;54:21-9.

[44] de Vries R. Depletion-induced instability in protein-DNA mixtures: Influence of protein charge and size. J Chem Phys. 2006;125.

[45] de Vries R. DNA compaction by nonbinding macromolecules. Polym Sci Ser C+. 2012;54:30-5.

[46] Zinchenko A, Tsumoto K, Murata S, Yoshikawa K. Crowding by Anionic Nanoparticles Causes DNA Double-Strand Instability and Compaction. J Phys Chem B. 2014;118:1256-62.

[47] Goodrich GP, Helfrich MR, Overberg JJ, Keating CD. Effect of macromolecular crowding on DNA : Au nanoparticle bioconjugate assembly. Langmuir. 2004;20:10246-51.

[48] Khimji I, Shin J, Liu JW. DNA duplex stabilization in crowded polyanion solutions. Chem Commun. 2013;49:1306-8.

[49] Spink CH, Chaires JB. Selective stabilization of triplex DNA by poly(ethylene glycols). J Am Chem Soc. 1995;117:12887-8.

[50] Nakano S, Karimata H, Ohmichi T, Kawakami J, Sugimoto N. The effect of molecular crowding with nucleotide length and cosolute structure on DNA duplex stability. J Am Chem Soc. 2004;126:14330-1.

[51] Feng B, Frykholm K, Norden B, Westerlund F. DNA strand exchange catalyzed by molecular crowding in PEG solutions. Chem Commun. 2010;46:8231-3.

[52] Uemura H, Ichikawa M, Kimura Y. Crossover behavior in static and dynamic properties of a single DNA molecule from three to quasi-two dimensions. Phys Rev E. 2010;81.

[53] Tang J, Levy SL, Trahan DW, Jones JJ, Craighead HG, Doyle PS. Revisiting the Conformation and Dynamics of DNA in Slitlike Confinement. Macromolecules. 2010;43:7368-77.

[54] Lee J, Kim S, Jeong H, Jung GY, Chang R, Chen YL, et al. Nanoslit Confined DNA at Low Ionic Strengths. Acs Macro Lett. 2014;3:926-30.

[55] van der Maarel JRC, Zhang C, van Kan JA. A Nanochannel Platform for Single DNA Studies: From Crowding, Protein DNA Interaction, to Sequencing of Genomic Information. Isr J Chem. 2014;54:1573-88.

[56] Reisner W, Morton KJ, Riehn R, Wang YM, Yu ZN, Rosen M, et al. Statics and dynamics of single DNA molecules confined in nanochannels. Phys Rev Lett. 2005;94.

[57] Persson F, Utko P, Reisner W, Larsen NB, Kristensen A. Confinement Spectroscopy: Probing Single DNA Molecules with Tapered Nanochannels. Nano Lett. 2009;9:1382-5.

[58] Reisner W, Beech JP, Larsen NB, Flyvbjerg H, Kristensen A, Tegenfeldt JO. Nanoconfinement-enhanced conformational response of single DNA molecules to changes in ionic environment. Phys Rev Lett. 2007;99.

[59] Zhang C, Zhang F, van Kan JA, van der Maarel JRC. Effects of electrostatic screening on the conformation of single DNA molecules confined in a nanochannel. J Chem Phys. 2008;128.

[60] Jo K, Dhingra DM, Odijk T, de Pablo JJ, Graham MD, Runnheim R, et al. A single-molecule barcoding system using nanoslits for DNA analysis. P Natl Acad Sci USA. 2007;104:2673-8.

[61] Kim Y, Kim KS, Kounovsky KL, Chang R, Jung GY, dePablo JJ, et al. Nanochannel confinement: DNA stretch approaching full contour length. Lab Chip. 2011;11:1721-9.

[62] Zhang C, Jiang K, Liu F, Doyle PS, van Kan JA, van der Maarel JRC. A nanofluidic device for single molecule studies with in situ control of environmental solution conditions. Lab Chip. 2013;13:2821-6.

[63] Yoshikawa K, Nomura SM, Tsumoto K, Takiguchi K. Construction of an In Vitro Model of a Living Cellular System. Minimal Cell: The Biophysics of Cell Compartment and Origin of Cell Functionality. 2011:173-93.

[64] Hamada T, Yoshikawa K. Cell-Sized Liposomes and Droplets: Real-World Modeling of Living Cells. Materials. 2012;5:2292-305.

[65] Dimitriadis GJ. Entrapment of Plasmid DNA in Liposomes. Nucleic Acids Res. 1979;6:2697-705.

[66] Fraley RT, Fornari CS, Kaplan S. Entrapment of a Bacterial Plasmid in Phospholipid-Vesicles - Potential for Gene-Transfer. P Natl Acad Sci USA. 1979;76:3348-52.

[67] Sato Y, Nomura SM, Yoshikawa K. Enhanced uptake of giant DNA in cell-sized liposomes. Chem Phys Lett. 2003;380:279-85.

[68] Nomura SIM, Tsumoto K, Yoshikawa K, Ourisson G, Nakatani Y. Towards proto-cells: "Primitive" lipid vesicles encapsulating giant DNA and its histone complex. Cell Mol Biol Lett. 2002;7:245-6.

[69] Sollogoub M, Guieu S, Geoffroy M, Yamada A, Estevez-Torres A, Yoshikawa K, et al. Photocontrol of single-chain DNA conformation in cell-mimicking microcompartments. Chembiochem. 2008;9:1201-6.

[70] Nomura S, Tsumoto K, Hamada T, Akiyoshi K, Nakatani Y, Yoshikawa K. Gene expression within cell-sized lipid vesicles. Chembiochem. 2003;4:1172-5.

[71] Tsumoto K, Nomura SM, Nakatani Y, Yoshikawa K. Giant liposome as a biochemical reactor: Transcription of DNA and transportation by laser tweezers. Langmuir. 2001;17:7225-8.

[72] Tresset G, Cheong WCD, Lam YM. Role of multivalent cations in the self-assembly of phosphiolipid-DNA complexes. J Phys Chem B. 2007;111:14233-8.

[73] Kato A, Shindo E, Sakaue T, Tsuji A, Yoshikawa K. Conformational Transition of Giant DNA in a Confined Space Surrounded by a Phospholipid Membrane. Biophys J. 2009;97:1678-86.

[74] Hamada T, Fujimoto R, Shimobayashi SF, Ichikawa M, Takagi M. Molecular behavior of DNA in a cell-sized compartment coated by lipids. Phys Rev E. 2015;91.

[75] Kato A, Yanagisawa M, Sato YT, Fujiwara K, Yoshikawa K. Cell-Sized confinement in microspheres accelerates the reaction of gene expression. Sci Rep-Uk. 2012;2.

[76] Jones JJ, van der Maarel JRC, Doyle PS. Effect of Nanochannel Geometry on DNA Structure in the Presence of Macromolecular Crowding Agent. Nano Lett. 2011;11:5047-53.

[77] Zhang C, Gong ZY, Guttula D, Malar PP, van Kan JA, Doyle PS, et al. Nanouidic Compaction of DNA by Like-Charged Protein. J Phys Chem B. 2012;116:3031-6.

[78] Biswas N, Ichikawa M, Datta A, Sato YT, Yanagisawa M, Yoshikawa K. Phase separation in crowded micro-spheroids: DNA-PEG system. Chem Phys Lett. 2012;539:157-62.

[79] Negishi M, Sakaue T, Takiguchi K, Yoshikawa K. Cooperation between giant DNA molecules and actin filaments in a microsphere. Phys Rev E. 2010;81.

[80] Negishi M, Ichikawa M, Nakajima M, Kojima M, Fukuda T, Yoshikawa K. Phase behavior of crowded like-charged mixed polyelectrolytes in a cell-sized sphere. Phys Rev E. 2011;83.

Figures

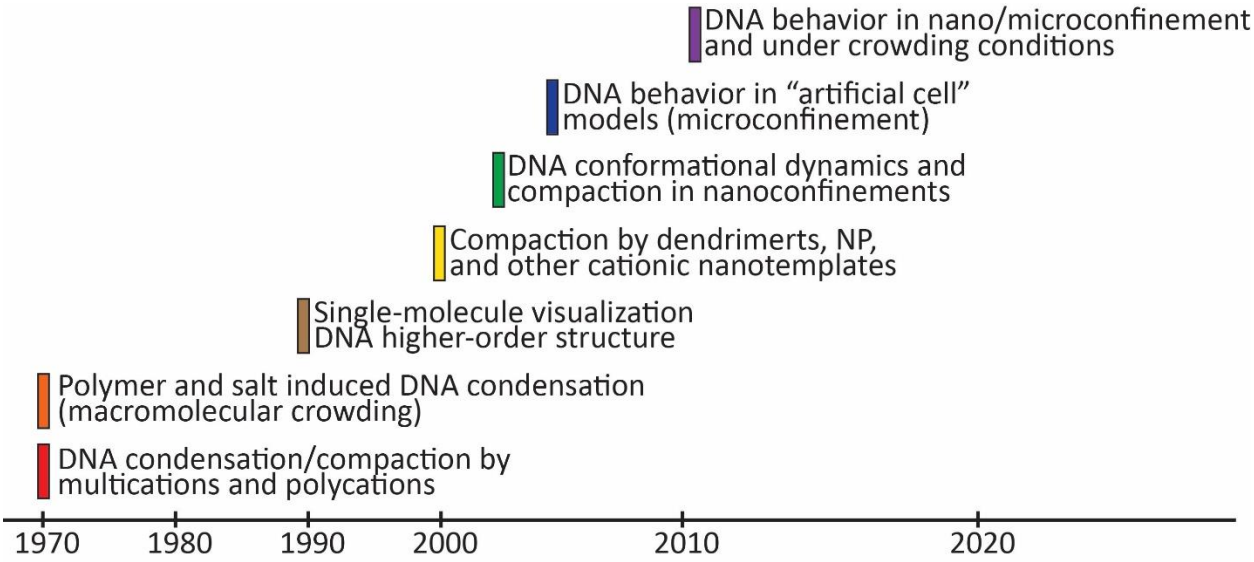

Figure 1.

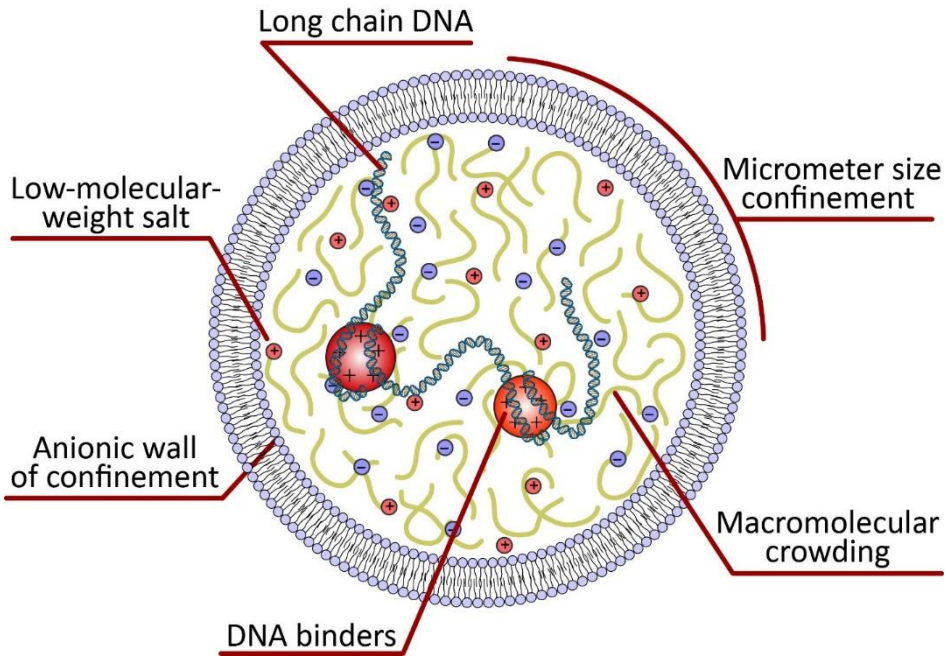
Long chain DNA
Micrometer size confinement
Low-molecular-weight salt
Anionic wall of confinement
Macromolecular crowding
DNA binders

Figure 2.

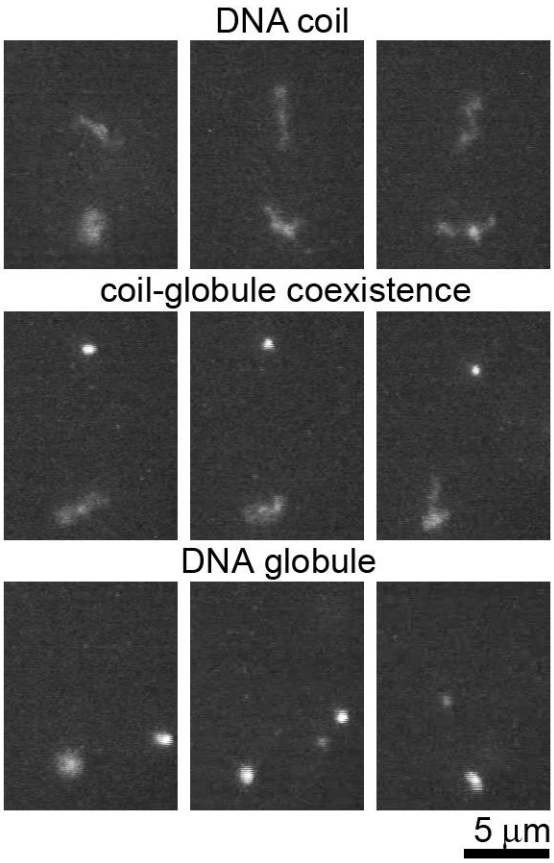

Figure 3.

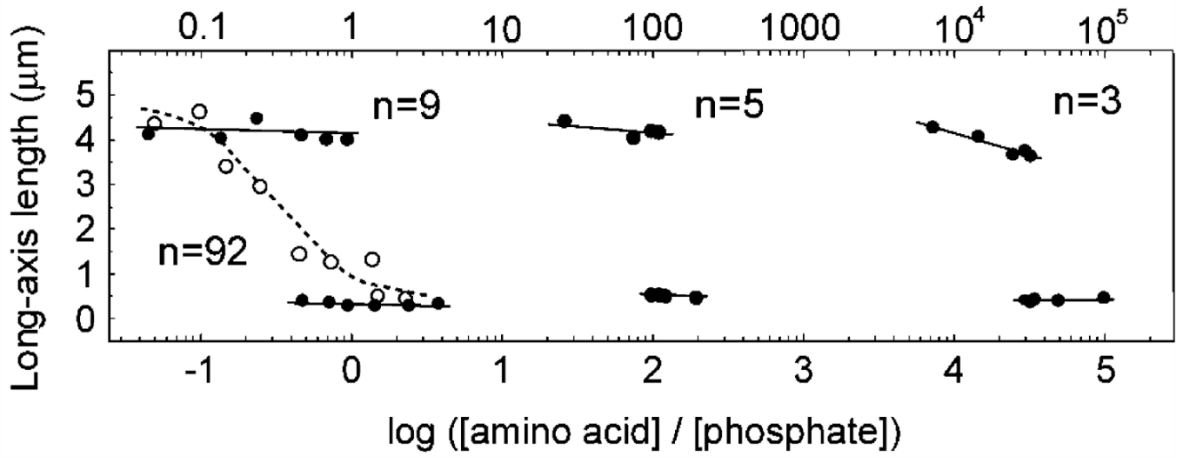
0.1
1
10
100
1000
10^4
10^5
Long-axis length (μm)
0
1
2
3
4
5
n=9
n=5
n=3
n=92
-1
0
1
2
3
4
5
log ([amino acid] / [phosphate])

Figure 4.

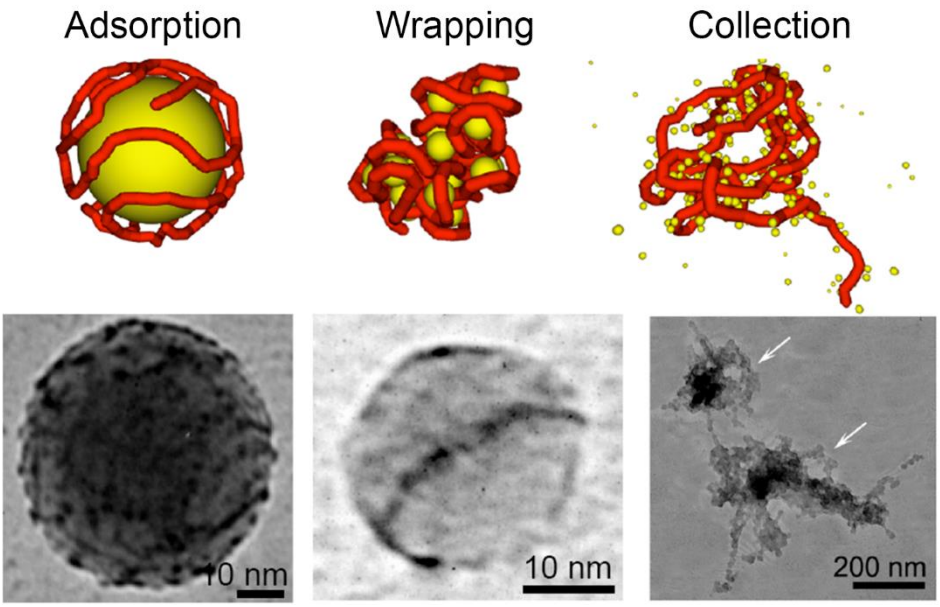

Figure 5.

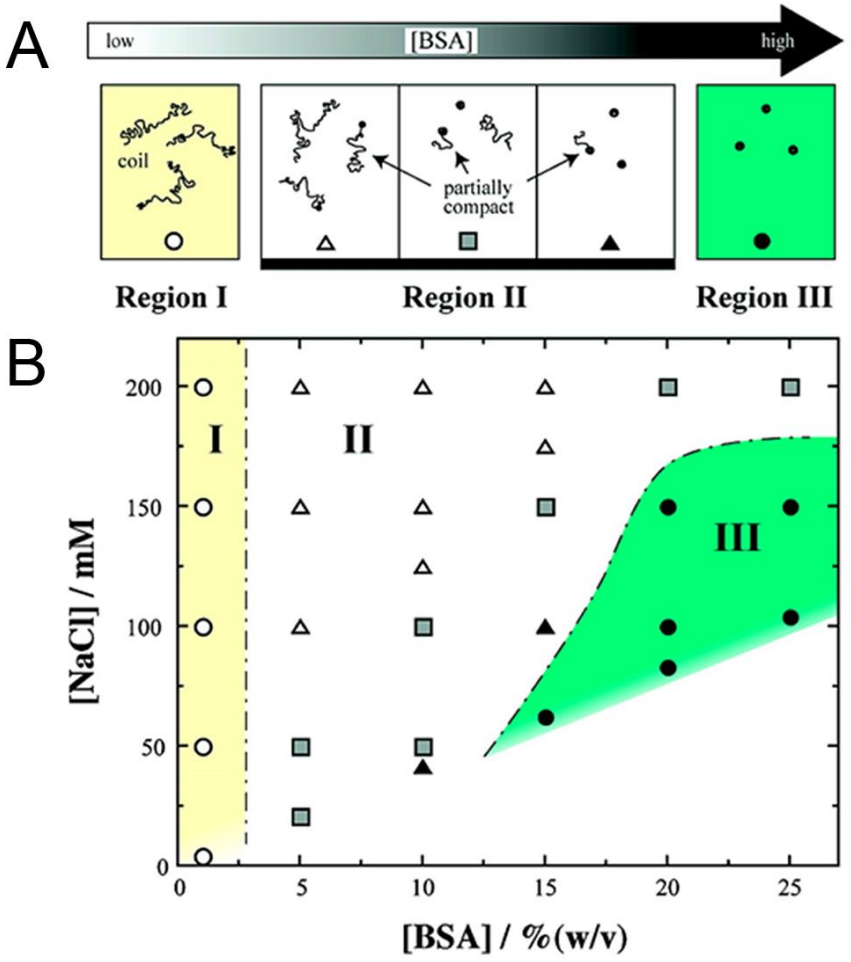
A
low
[BSA]
high
coil
partially
compact
Region I
Region II
Region III
B
I
II
III
[NaCl] / mM
[BSA] / %(w/v)
0
50
100
150
200
0
5
10
15
20
25

Figure 6.

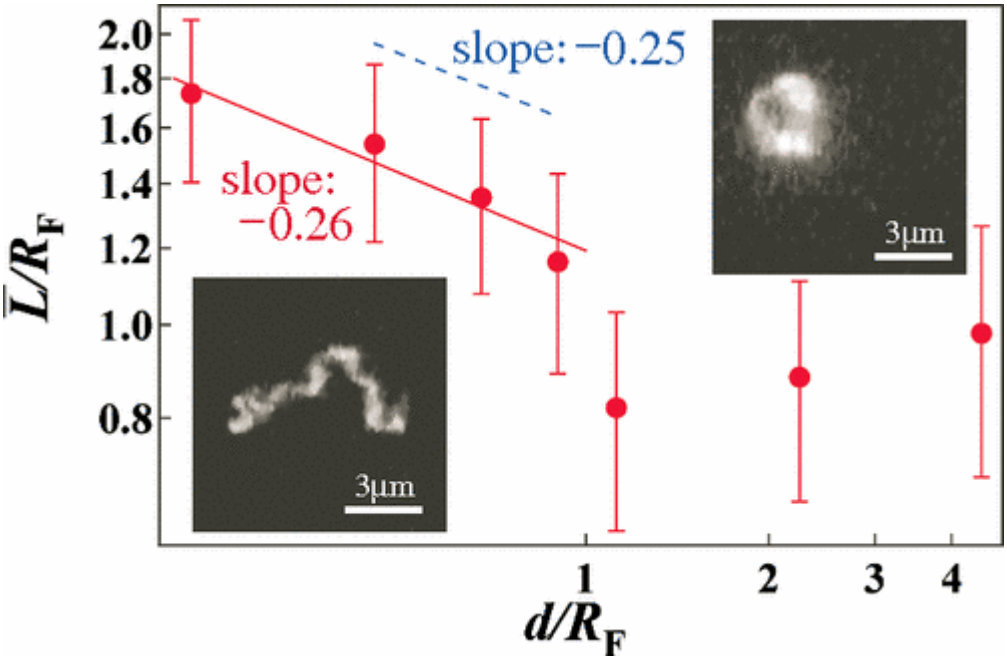
2.0
1.8
1.6
1.4
1.2
1.0
0.8
$\overline{L}/R_F$
slope: −0.25
slope:
−0.26
3μm
3μm
1
2
3
4
d/R_F

Figure 7.

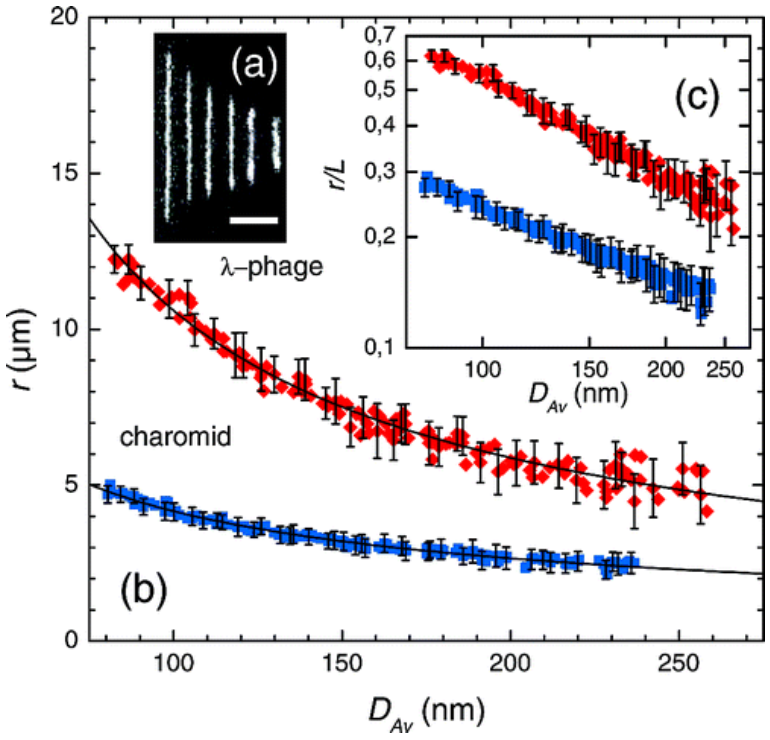

Figure 8.

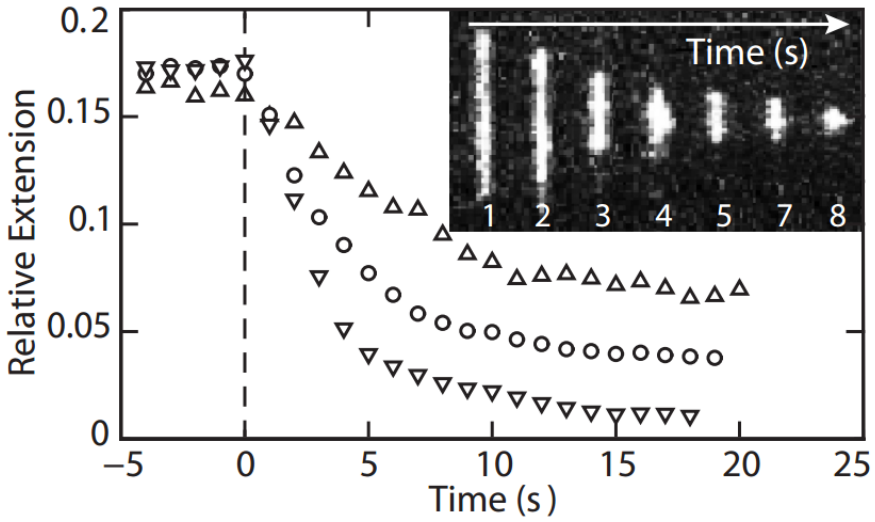
0.2
0.15
0.1
0.05
0
Relative Extension
−5
0
5
10
15
20
25
Time (s)
Time (s)
1
2
3
4
5
7
8

Figure 9.

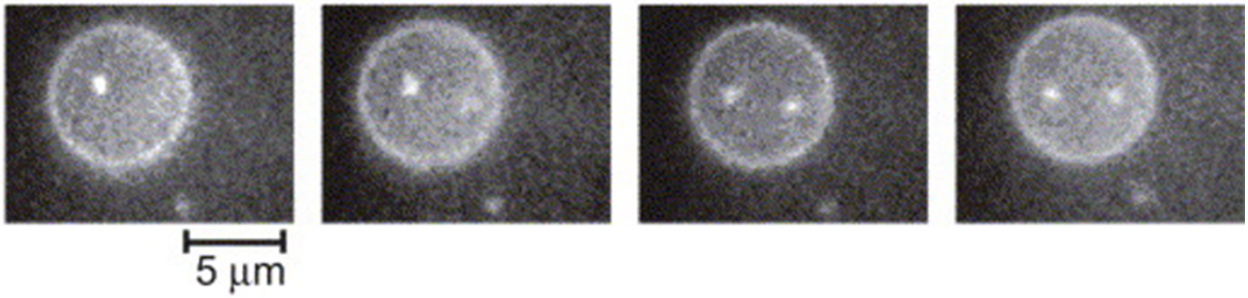

Figure 10.

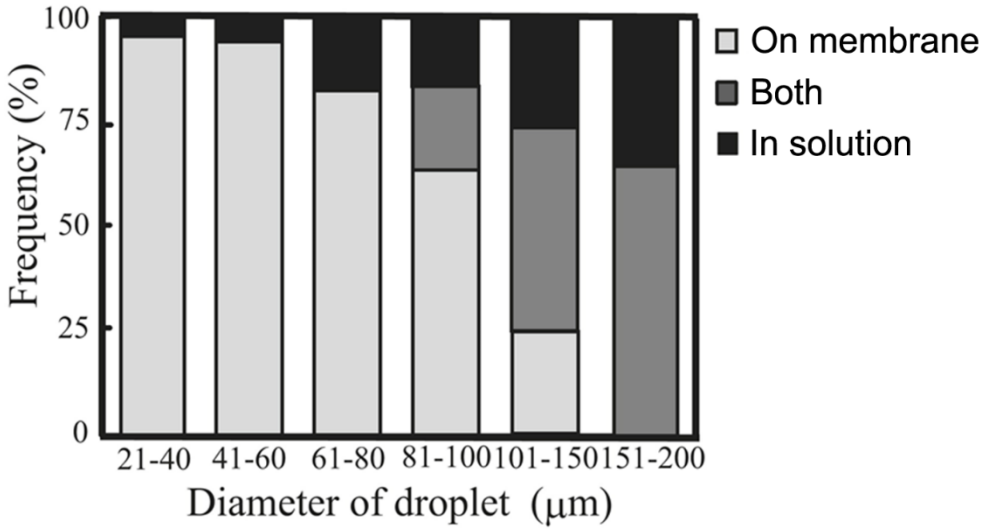
100
75
50
25
0
Frequency (%)
21-40
41-60
61-80
81-100
101-150
151-200
Diameter of droplet (μm)
On membrane
Both
In solution

Figure 11.

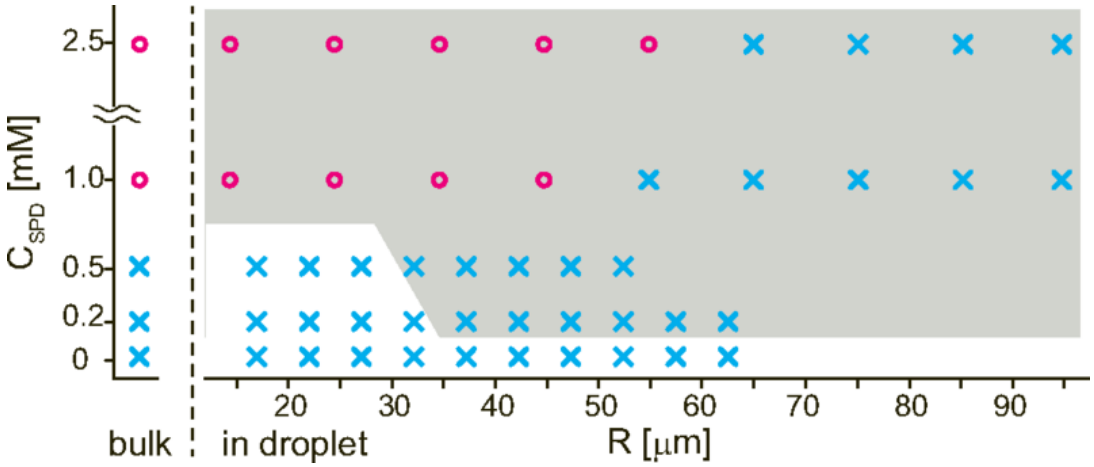

Figure 12.

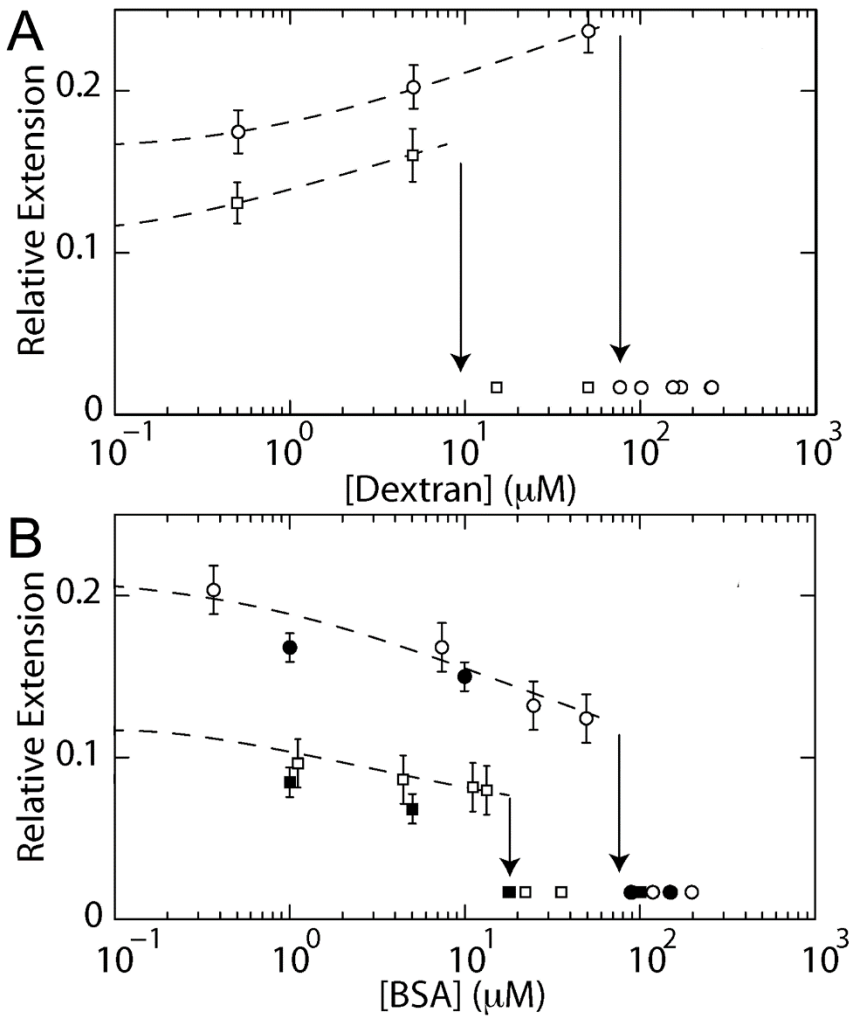
A
Relative Extension
0.2
0.1
0
10^{-1}
10^{0}
10^{1}
10^{2}
10^{3}
[Dextran] (μM)
B
Relative Extension
0.2
0.1
0
10^{-1}
10^{0}
10^{1}
10^{2}
10^{3}
[BSA] (μM)

Figure 13.

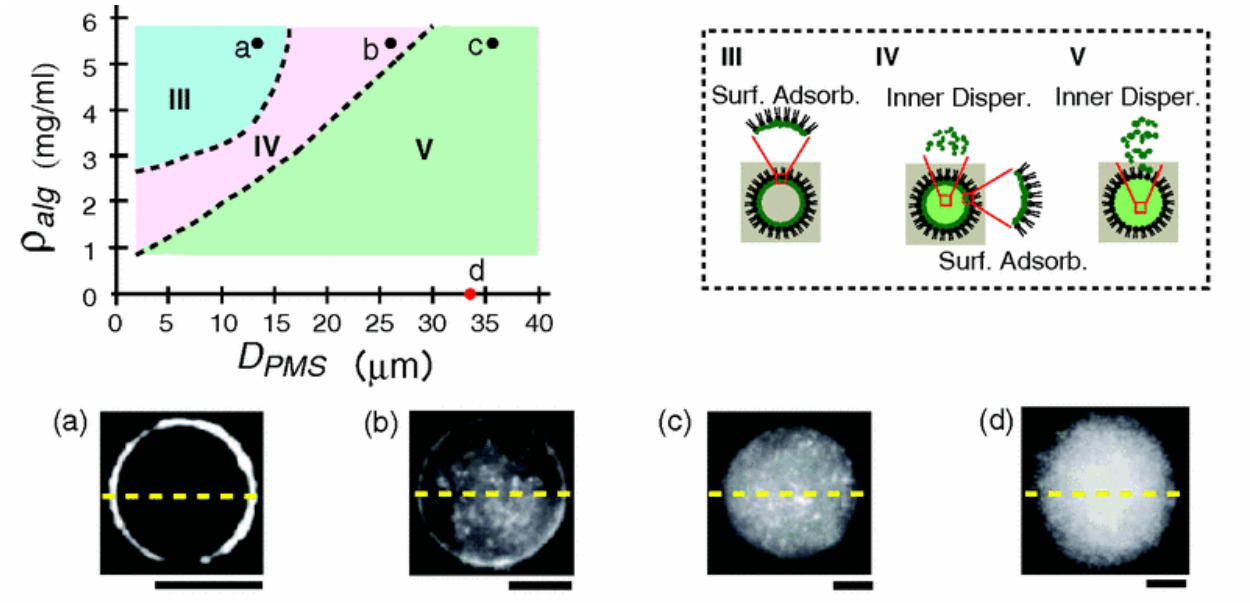
ρalg (mg/ml)
DPMS (μm)
a
b
c
d
III
IV
V
Surf. Adsorb.
Inner Disper.
Inner Disper.
Surf. Adsorb.
(a)
(b)
(c)
(d)

Figure 14.

Figure Captions

Figure 1. Timeline (not to scale) of studies in the field of DNA condensation.

Figure 2. Artificial cell model showing the complexity of an experimental system simultaneously taking into account the micrometer size of DNA confinement and the confinement wall effects, crowded environment inside the confinement, interaction of DNA with various types of cationic binders, and the presence of high concentrations of surrounded ions.

Figure 3. Single-molecule observation of T4 DNA (165 kbp, *ca.* 60 μm contour length) compaction by spermine. Representative fluorescence microscopy images of dye-labeled T4 DNA molecules in coil, globule, and coil-globule coexistence conformational states.**Figure 4.** Change in the long-axis length of T4 DNA (0.2 μM) macromolecule as a function of the poly-l-lysine concentration. The horizontal axis shows the charge ratio between poly-l-lysine (amino groups) and T4 DNA (phosphates). The numbers *n* for each dependence correspond to the number of residues in the poly-l-lysine used for DNA compaction. Open circle represents the average for all DNA molecules in the given condition. Values shown by closed circles represent the average values for DNA in coil and globule state, respectively. (Adapted from [13])

Figure 5. Three modes of DNA interaction with cationic nanoparticles. Typical snapshots obtained from molecular dynamics simulations of single-chain DNA fully compact state for large, medium, and small nanoparticles and transmission electron microscopy images of the DNA complexes with nanoparticles of *ca.* 100 nm, 25 nm, and 10 nm. (Adapted from [21, 22])

Figure 6. (**A**) Schematic representation of the change in the higher-order structure of DNA with an increase in the BSA concentration. Regions I and III are the extreme states in which all DNA molecules exhibit the elongated coil and fully compact conformations, respectively. Region II

shows the intermediate state, which includes intrachain segregated conformation, as depicted schematically. Partially compacted DNA molecules only exist in region II. (**B**) Phase diagram of the conformation of DNA as a function of the NaCl and BSA concentrations. (Adapted from [42])

Figure 7. Dependence of the average major length of a DNA molecule L on the thickness of a slit d. Both L and d are represented in the normalized scale by the Flory radius in three dimensions, R_F=4.45 μm. The fluorescent images in a thin (left: d = 1 μm) and a thick cell (right: d = 10 μm) are also presented.

Figure 8. (a) Fluorescence images of λ-DNA molecule confined at different spatial positions along the same tapered nanochannel. The geometric average increases in from left to right: $D_{Av}\approx$ 97, 118, 155, 194, 215, 240 nm, respectively. The scale bar is 5 μm. (b) Molecule extension r as a function of geometric average D_{Av} measured for linear λ-DNA (upper trace, 48.5 kbp, $L_{10:1}$ = 19.8 μm) and circular charomid DNA (lower trace, 42.2 kbp, $L_{10:1}$ = 17.2 μm). (Adapted from [57])

Figure 9. Compaction of T4 DNA following exposure to a solution of 1 (upper curve), 3 (middle curve) and 5 (lower curve) μM protamine in 1×T buffer. The DNA molecules are confined in channels with a cross-section of 200 × 250 nm^2. The data represent average trajectories pertaining to the compaction of five different molecules. The inset shows a time-lapse series of fluorescence images pertaining to the compaction following exposure to 5 μM protamine in 1×T buffer. Time zero is defined as the moment when the molecules start to compact. (Adapted from [62])

Figure 10. Fluorescent microscopic images of a giant liposome entrapping a couple of T4 DNA molecules. (Adapted from [67])

Figure 11. Dependence of the T4 DNA distribution on droplet-size in DOPE microdroplets. DOPE microdroplets encapsulating T4 DNA with 10 mM Mg^{2+} and 1.5 mM spermine were observed under confocal microscopy. (Adapted from [73])

Figure 12. Phase diagram of DNA behavior in droplets as a function of droplet radius R and spermidine concentration C_{SPD}. Crosses and circles indicate coil and globular conformations of DNA, respectively. Gray region corresponds to the adsorption of DNA on the membrane surface. (Adapted from [74])

Figure 13. (**A**) Relative extension of T4 DNA versus the concentration of dextran (M_w = 50 kDa) in 300 × 300 nm^2 (circle) and 200 × 300 nm^2 (square) channels. For all panels, the buffers are 10 mM Tris/HCl (circle) or 10 mM Tris/HCl with 25 mM NaCl (square). (**B**) Relative extension T4 DNA (open symbols, YOYO-1 stained) and λ-DNA (closed symbols, Alexa stained) versus the concentration of BSA in 200 × 300 nm^2 channels. (Adapted from [77])

Figure 14. (top) Phase diagram of the DNA distribution in phospholipid-coated micrometer-scale closed sphere (PMS) containing 0.34 mg/mL of DNA and various amounts of alginate. Schematic illustrations of the DNA distribution is shown in the right rectangle. (bottom) Representative fluorescence microscopic images of DNA localization in the PMSs, where labels a–d refer to the corresponding conditions in the phase diagram. Scale bars are 10 μm. (Adapted from [80])